dicarbonyl resides within the zeolite framework. The most likely position is the α cage since the β cage is inaccessible to even the smallest phosphine used, i.e. $P(CH_3)_2(C_6H_5)$. Rhodium clusters **1** generated from Rh(OH)-Z, appear to reside on the surface of the zeolite particle by similar reactions. Gelin et al.[1] and Mantovani et al.[6] conclude that rhodium clusters formed by their methods reside in the α cage. The observed stretching frequencies in their preparations are shifted significantly from those obtained for **1** and for pure $Rh_6(CO)_{16}$ (in particular, the bridging carbonyl frequency is shifted to 1770 cm^{-1}). This may reflect a site for **1** at or near the surface of the zeolite.

The reaction of $Rh(CO)_2^+$ (**5**) with large phosphines at 120 °C establishes that the dicarbonyl is sufficiently mobile to migrate to the surface at this temperature. The large phosphines, particularly triphenylphosphine, are much larger than the channel dimension of 13X.

At this point the differences in carbonylation chemistry of Rh(OH)-Z and $Rh(NH_3)$-Z as outlined in Figures 1 and 3 are not clear. We speculate that the two exchange procedures place rhodium at different sites in the zeolite; this may result from the differences in pH in the two exchange methods.

Acknowledgment. We thank Dr. John Yamanis of Allied Corp. for many helpful discussions concerning this work and Dr. John Dillard for help with the XPS experiments. Financial support for this work was provided by the Jeffress Memorial Trust. E.R. wishes to thank Tennessee Eastman for a predoctoral fellowship.

Registry No. $Rh(CO)_2^+$, 88129-88-8; $Rh(CO)(P(EtCN)_3)^+$, 88129-89-9; $Rh(CO)_2(DPM)^+$, 88129-90-2; $Rh(CO)DPM^+$, 88129-91-3; $Rh_6(CO)_{16}$, 28407-51-4; CO, 630-08-0; H_2, 1333-74-0.

Contribution from the Istituto per lo Studio della Stereochimica ed Energetica dei Composti di Coordinazione, CNR, 50132 Florence, Italy, and Department of Chemistry, Cornell University, Ithaca, New York 14853

A Molecular Orbital Analysis of the Bonding Capabilities of Carbon Disulfide and Carbon Dioxide toward Transition-Metal Fragments

CARLO MEALLI,*[1a] ROALD HOFFMANN,*[1b] and ARMEL STOCKIS[1c]

Received March 2, 1983

The bonding to transition-metal fragments of heteroallene type molecules such as CS_2 and CO_2 is investigated by using the extended Hückel method. When a linear CX_2 molecule and a transition-metal fragment are brought together, the metal atom can either lie in a direction collinear with the X-C-X vector (end-on approach) or lie perpendicular to it (side-on approach). The possible routes that, departing from these two alternative geometries at the *rendezvous* time, subsequently lead to the η^2 coordination of CX_2 have been traced. The calculations show that the reaction path that starts from end-on is energetically most accessible. The C coordination of CO_2, once observed in a cobalt(I) complex, has been considered, and arguments for the stability of this geometry are presented. The paper also deals with the fluxionality processes found in some complexes and offers suggestions as to how one can interpret some of the reactivities of complexed CO_2 and CS_2 molecules.

The coordination properties of triatomics such as CS_2, CO_2, and COS are interesting, especially from a synthetic viewpoint. The ultimate goal is the activation of carbon dioxide, which is potentially the most abundant source of C_1 chemistry. It may be reasonably expected that the activation process proceeds through transition-metal catalysis. In spite of the great efforts devoted to this field, the ascertained coordination of these molecules to transition metals is limited to a restricted number of compounds.[2]

The big problem is that of magnifying the meager bonding capabilities of these triatomic molecules, an operation which will be ensured of success only if the bonding is understood in detail in terms of simple and useful constructs.

From a theoretical point of view the literature is full of qualitative suggestions as to how one should interpret the electronic structure of these compounds;[3] quantitatively, however the number of MO investigations is very limited.[4] Recently, a very nice MO initio study of the models $(PH_3)_2NiCO_2$ and $(PH_3)_2CuCO_2^+$ has appeared.[5] The authors, after investigating several modes of coordination, confirm the validity of the Chatt-Dewar-Duncanson model for metal-olefin complexes when applied to η^2-bonded carbon dioxide molecules. In particular they underline the contribution of electrostatic terms to the total energy. When the metal atom is positively charged, this term dominates and CO_2 may prefer end-on to side-on coordination. On the basis of the latter argument itself, the extended Hückel method[6] may appear rather inadequate for the interpretation of the bonding in these compounds. However, the relative facility with which the calculations can be repeated and the use of the fragment orbital formalism[7] make the EH method still attractive. In particular, many numerical experiments can be made to learn how a metal fragment and a linear triatomic molecule of the type CX_2 can be brought together. After the initial *rendezvous*, we can follow the possible geometrical rearrangment pathways that lead to the different coordination modes experimentally observed.

Definition of the Geometrical Parameters

It is widely accepted that there are three possible modes of coordination of CS_2 or CO_2 molecules to a single metal function. Detailed structural evidence exists for mode **1**,[8]

(1) (a) Istituto Stereochimica. (b) Cornell University. (c) Laboratoire de Chimie Organique, Université de Liege, Liege, Belgium.
(2) See the following review articles, summarizing the most recent literature: (a) Butler, I. S.; Fenster, A. E. *J. Organomet. Chem.* **1974**, *66*, 161. (b) Volpin, M. E.; Kolomnikov, I. S. *Organomet. React.* **1975**, *5*, 313. (c) Yaneff, P. V. *Coord. Chem. Rev.* **1977**, *23*, 183. (d) Kolomnikow, I. S.; Grigoryan, M. Kh. *Russ. Chem. Rev. (Engl. Transl.)* **1978**, *47*, 603. (e) Eisenberg, R.; Hendricksen, D. E. *Adv. Catal.* **1979**, *28*, 119. (f) Ibers, J. A. *Chem. Soc. Rev.* **1982**, *11*, 1. (g) Werner, H. *Coord. Chem. Rev.* **1982**, *43*, 165.
(3) (a) LeBozec, H.; Dixneuf, P. H.; Carty, A. J.; Taylor, N. J. *Inorg. Chem.* **1978**, *17*, 2568. (b) Conway, P.; Grant, S. M.; Manning, A. R. *J. Chem. Soc., Dalton Trans.* **1979**, 1920.
(4) (a) Sakaki, S.; Kudou, N.; Ohyoshi, A. *Inorg. Chem.* **1977**, *16*, 202. (b) Demoulim, D.; Pullmann, A. *Theor. Chim. Acta* **1978**, *49*, 161. (c) Ozin, G. A.; Huber, H.; McIntosh, D. *Inorg. Chem.* **1978**, *17*, 1472.
(5) Sakaki, S.; Kitaura, K.; Morokuma, K. *Inorg. Chem.* **1982**, *21*, 760.
(6) Hoffmann, R.; Lipscomb, W. N. *J. Chem. Phys.* **1962**, *36*, 2179, 3489; **1962**, *37*, 2878. Hoffmann, R. *Ibid.* **1963**, *39*, 1397.
(7) (a) Hoffmann, R.; Fujimoto, H.; Swenson, J. R.; Wan, C.-C. *J. Am. Chem. Soc.* **1973**, *95*, 7644. (b) Fujimoto, H.; Hoffmann, R. *J. Phys. Chem.* **1974**, *78*, 1167.

0020-1669/84/1323-0056$01.50/0

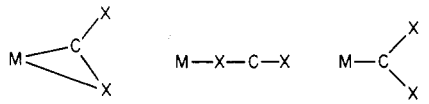

1 2 3

whereas only one example where CO_2 is coordinated as in **3** is known: **4**.[9] Finally, modes **2** and **3** are proposed from spectroscopic evidence.[10]

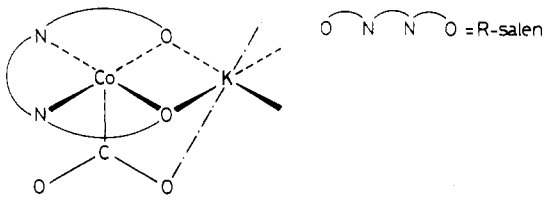

4

There are two natural ways of approaching a linear X–C–X molecule to a metal fragment. In the first case, the metal atom lies collinear with the X–C–X vector, as shown in **5**. This

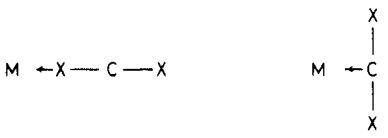

5 6

reaction path leads directly to mode **2** or end-on coordination. Alternatively the approach can be in a direction perpendicular to the X–C–X axis. **6** seems to be the least motion pathway leading to mode **3** when combined with a bending of the CX_2 molecule. Now the question is whether the common mode **1** is obtainable through a rearrangment of mode **2** or through a rearrangment of mode **3**. We outline two alternative *routes* leading to η^2 coordination of a CX_2 type of molecule to a metal fragment.

The first step of *route I* consists of slipping the carbon atom, coordinated initially as in **3**, off the main axis of the metal fragment, e.g. the threefold axis of L_3M fragments or the twofold axis of L_2M fragments. Since the calculations are known to be sensitive to bond distance variations, the M–C length is fixed and the slipping-off motion is defined as a function of the angular parameter θ, **7**. However, the angle

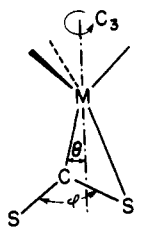

7

θ and the angle φ, which defines the amount of bending of the CX_2 molecule, do not suffice to reproduce the experimental geometry found, for example, in a complex such as (triphos)$CoCS_2$[7g] (**1**) [triphos = $CH_3C(CH_2PPh_2)_3$] where θ is $\sim$28° and φ is 133.8°. In fact, unlike **7**, the bisector of the φ angle is not exactly parallel to the (triphos)Co pseudo-threefold axis but forms an angle of about 6°. In our model, the latter angular parameter is defined in **8**. The spindle axis of the β rotation is normal to the plane of the drawing, which is also a mirror plane for the molecule and passes through the carbon atom.

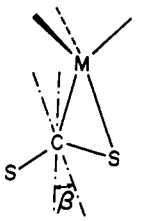

8

In summary, *route I* from **3** to **1** is achieved through a combined variation of the angles θ, φ, and β.

Alternatively, mode **1** can be accessed from mode **2** through *route II*, whose angular parameters can be defined as follows: a rotation of the linear molecule X–C–X with respect to the main axis of the metal fragment. This rotation, defined in **9**

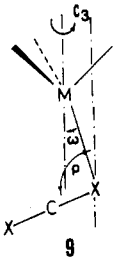

9

as ρ, can be accompanied by a slipping motion of CX_2 off the metal fragment main axis. This movement is better defined in terms of an angular parameter, ω, if we want to keep the M–X bond distance unchanged. An increase in ω and a decrease in ρ shorten the M–C distance to a point where the carbon atom is also bound to the metal. It is possibly then that the CX_2 molecule starts kinking, as shown in **10**. Again,

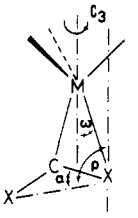

10

in order not to bias the calculations the C–X distances were kept fixed during the kinking motion defined by the rotation α. Notice that for any α the X–C–X angle is defined as 180° – 2α. The experimental structure of **1** has ω, ρ, and α values of ca. 18, 97, and 22°, respectively.

After defining the two reaction paths, we tried both route I and route II computationally in order to learn which one is energetically more probable.

Formation of M–CS_2 η^2 Linkages

Route I. Figure 1 shows an interaction diagram for a model compound, $(PH_3)_3NiCS_2$, tht has the conformation shown in **3**. The θ and φ angular parameters defined in **7** were fixed at 0 and 150°, respectively, whereas the Ni–C and C–S distances were fixed at 1.90 and 1.60 Å, respectively. At the right

(8) (a) Kashiwagi, T.; Yasuoka, N.; Ueki, T.; Kasai, N.; Kakudo, M.; Takahashi, S.; Hagihara, N. *Bull. Chem. Soc. Jpn.* **1968**, *41*, 296. (b) Mason, R.; Rae, A. I. M. *J. Chem. Soc. A* **1970**, 1767. (c) Drew, M. G. B.; Pu, L. S. *Acta Crystallogr., Sect. B* **1977**, *B33*, 1207. (d) LeBozec, H.; Dixneuf, P. H.; Carty, A. J.; Taylor, N. J. *Inorg. Chem.* **1978**, *17*, 2568. (e) Werner, H.; Leonhard, K.; Burschka, Ch. *J. Organomet. Chem.* **1978**, *160*, 291. (f) Facchinetti, G.; Floriani, C.; Chiesi-Villa, A.; Guastini, C. *J. Chem. Soc., Dalton Trans.* **1979**, 1612. (g) Bianchini, C.; Mealli, C.; Meli, A.; Orlandini, A.; Sacconi, L. *Inorg. Chem.* **1980**, *19*, 2968.

(9) (a) Facchinetti, G.; Floriani, C.; Zanazzi, P. F. *J. Am. Chem. Soc.* **1978**, *100*, 7405. (b) Gambarotta, S.; Arena, F.; Floriani, C.; Zanazzi, P. F. *Ibid.* **1982**, *104*, 5082.

(10) Werner, H.; Bertleff, W. *Chem. Ber.* **1980**, *113*, 267. See also ref 2c and references therein.

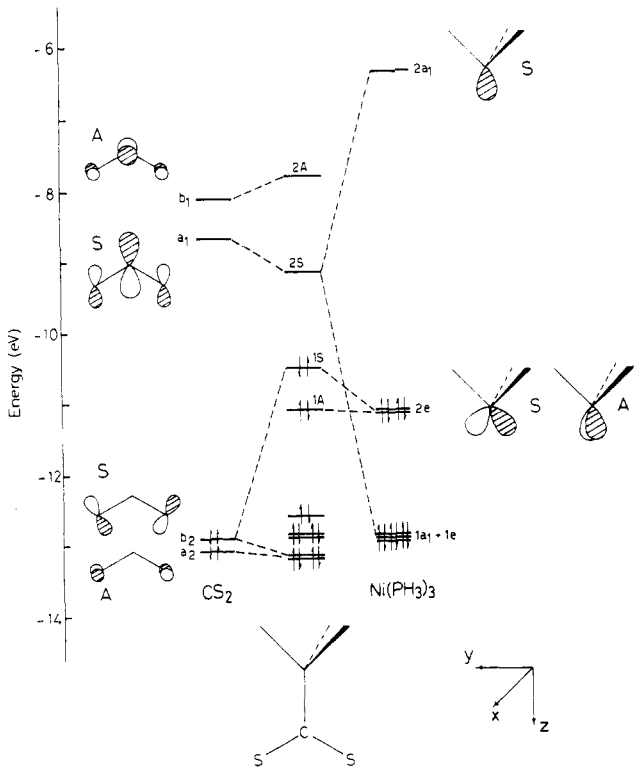

Figure 1. Interaction diagram for the molecular model $(PH_3)_3NiCS_2$. The CS_2 molecule is bent and bonded through the carbon atom to the metal. The molecular symmetry is C_s.

of Figure 1 the known orbitals of a L_3M fragment are illustrated.[11] There are three low-lying filled orbitals that are the remnants of the octahedral t_{2g} set; at higher energy the hybrid 2e orbitals (the labels are appropriate for C_{3v} symmetry) which in the case of the d^{10} nickel atom are fully populated. Finally at high energy there is an empty metal sp hybrid. The reader is warned that during the discussion we will often switch from L_3M to L_2M fragments when dealing with d^{10} metals (in one case we will also refer to a d^9 species). d^8-L_4M and d^6-L_5M fragments will do as well because of their isolobal analogy.[11b,12] The reason is that all of these fragments are characterized by one filled metal hybrid orbital (the equivalent of the S member of the 2e level in Figure 1) and by one empty high-lying sp orbital. These are the orbitals appropriate for σ donation and π back-donation with side-on oriented CX_2 molecules, in analogy with the Chatt–Dewar–Duncanson description of metal–olefin bonding.

In Figure 1 four selected orbitals of a bent CS_2 molecule are shown at the left side. The labels are those of the C_{2v} point group. Notice that the lower b_2 and a_2 orbitals come from the π_g level of the linear CS_2 molecule, actually a combination of lone pairs at the sulfur atom.[13] The higher b_1 and a_1 empty orbitals descend from the π_u^* set of the linear molecule. When the complex is formed, only a mirror plane is maintained and the orbitals are classified as symmetric, S, or antisymmetric, A, with respect to this plane.

There is little bonding between the interacting fragments. A weak interaction is established between the metal d_{z^2} orbital ($1a_1$) and the CS_2 empty a_1 orbital. The interaction between the CS_2 b_2 orbital and the metal 2e S member is destabilizing, since both the interacting orbitals are filled. As a matter of

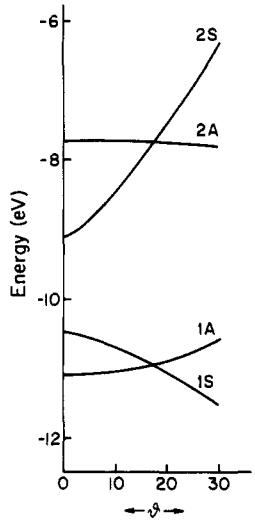

Figure 2. Evolution of the frontier orbitals of $(PH_3)_3NiCS_2$ for shifting a bent CS_2 molecule (S–C–S = 150°) off the threefold axis of the metal fragment.

fact the HOMO, which is the antibonding combination of metal and CS_2 b_2 orbitals, decreases in energy on decreasing the φ angle (see **7** for the definition of the angle) because of reduced overlap. A minimum of the total energy is found for $\varphi \sim 146°$. However a C-coordinated complex of this sort appears unstable, mainly because there is little donation from CS_2 to the metal on account of the electrophilic character of the carbon atom. Remenber that $(PH_3)_3Ni$ is a 16-electron species and that the donation of two electrons from a ligand is formally required to attain a stable closed-shell configuration. Analogously, a $(PH_3)_2Ni$ fragment requires two more electrons to attain the 16-electron configuration stable for square-planar complexes.[11b] The carbon atom itself cannot be a two-electron donor. In fact only the CS_2 S set, descending from π_u (not shown in Figure 1), seems apt to donation into the empty metal $2a_1$ orbital. However, because of the large energy gap between the interacting fragment orbitals and mainly because of the very slight contribution of carbon to π_u, the interaction is extremely weak. The composition of π_u derives from the difference of electronegativity between sulfur and carbon.[13]

We have then considered the slipping of CS_2 off the L_3M main axis. The θ and φ angles defined in **7** have been varied independently, but Figure 2 shows the evolution of the four upper orbitals of Figure 1 as a function of θ alone, the φ value being fixed at 150°. The five orbitals underneath those four reported in Figure 2 spread out a little but remain substantially compact. The important point is the repulsion between the two MOs of S symmetry since the slipping-off motion destroys the pseudosymmetry of these orbitals. The argument applies straightforwardly to L_2MCS_2 complexes where there is a true descent of symmetry from C_{2v} to C_s when θ starts deviating from a null value. Thus, the HOMO and LUMO (originally b_2 and a_1, respectively) start to repel each other on account of mixing, which magnifies both the bonding character of HOMO and the antibonding character of LUMO. **11** shows

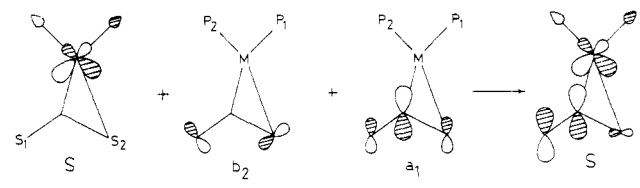

11

how this mixing occurs in HOMO for the L_2MCS_2 case, but

(11) (a) Dedieu, A.; Albright, T. A.; Hoffmann, R. *J. Am. Chem. Soc.* **1979**, *101*, 3141. (b) Albright, T. A. *Tetrahedron* **1982**, *38*, 1339.
(12) Hoffmann, R. *Angew. Chem., Int. Ed. Engl.* **1982**, *21*, 711.
(13) For a detailed description of the MOs in linear and bent AB_2 molecules see: Gimarc, B. M. "Molecular Structure and Bonding"; Academic Press: New York, 1979; p 153–169.

it is clear that the same picture holds also for L_3MCS_2 complexes. **11** also shows that the resulting MO contains a large percentage of an orbital of the uncoordinated sulfur atom. Thus, part of the electron density donated from the metal concentrates on the latter atom. Moreover the direction of the sulfur orbital in question is such that in adducts of the CS_2 compounds with a σ-oriented electrophilic agent, E, e.g. alkyl,[8f,g,14] $Cr(CO)_5$,[8g] or $Mn(CO)_2(C_5H_5)$,[15] the angle C–S–E assumes values in the range 100–120°.

Figure 2 clearly shows that in the case of L_3MCS_2 complexes there is a level crossing between the 1S and 1A levels; this changes the nature of the HOMO. Notice that for a complex such as **1**, which contains a d^9 metal, the crossing is formally forbidden. The crossing is not observed in L_2MCS_2 complexes since the equivalent of the level 1A, **12**, unhybri-

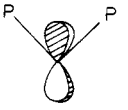

12

dized, is buried together with three other low-lying d orbitals. In any case these orbitals of A symmetry are metal centered; in fact we have found generally that π type interactions with opportune CS_2 π orbitals are rather scarce in these compounds.

Stimulated by these aspects of the theoretical analysis, we have carried out in parallel a structure determination of the nickel analogue of complex **1**, namely the compound (triphos)$NiCS_2$ (**2**).[16] The full crystallographic details will be reported elsewhere, but here we point out a result that confirms the analysis outlined above: there is no major structural variation in **2** compared to **1** that is likely to have been generated by electronic effects. Since **2** contains one electron more than **1**, we conclude that this extra electron is located in a nonbonding orbital centered on the metal. This is in accord with the predicted antisymmetric, primarily metallic nature of the HOMO. The absence of significant π interactions of this metal orbital with appropriate CS_2 π orbitals is also confirmed. More experimental evidence of the correct assignment of the HOMO is obtained from EPR measurements on complex **1**.[16] It is confirmed that the compound contains one unpaired electron located in an orbital that identifies better with the A rather than with the S member of the metal 2e set (see Figure 1).

Independent optimizations of the angular parameters θ and φ for both $(PH_3)_2NiCS_2$ and $(PH_3)_3NiCS_2$ models provided values of ca. 28 and 150°, respectively, in any case. The first value is close to the experimental value found in the structures of compounds **1** and **2** and other CS_2 complexes such as $(PPh_3)_2PtCS_2$[8b] (**3**), $(PPh_3)_2PdCS_2$[8a] (**4**), and $(PMe_3)(PPh_3)(CO)_2FeCS_2$[8d] (**5**) as well. Concerning the φ value, this is calculated 10–15° larger than the experiment. This fact suggests that the angle is sensitive to some specific energetic or geometrical parameter not properly accounted for by the present calculation. This is an important point that we will reexamine later in some detail.

Next we directed our attention to the rocking motion as a function of the β angle defined in **8**. Actually we did not consider β as a third independent variable, but the rocking of CS_2 was started after optimizing the angles θ and φ. The rocking motion is computed to be energetically soft in any case. Notice however that the motion mainly acts to reduce the metal–sulfur distance, and since the previously optimized φ angle is too large, the experimental distances are matched at an early stage of the β rotation. For $(PH_3)_2NiCS_2$ the optimized β is +8°,[17] to be compared with the experimental value of 12° in the structure of **3**. The main effect of rocking is to increase the overall bond order between the metal fragment and CS_2. The overlap population is increased by about 25% for L_2MCS_2 complexes and by about 10% for L_3MCS_2 complexes. About half of the increased bond order comes from a larger overlap between the filled metal S hybrid and the empty CS_2 a_1 orbital, which are both shown in **11**. This corresponds to a better metal–ligand π type back-bonding interaction, but also the ligand–metal σ type donation is improved when the angle between the fragment main axis and the coordinated C–S bond goes toward orthogonality.

There is another important effect of the rocking motion relating to the overall geometry of the complexes. In structures **3** and **4** but also in the CO_2 complex, $(PCy_3)_2NiCO_2$ (**6**),[18] the metal–phosphorus bond trans to the carbon atom is some 0.1 Å longer than the other M–P bond trans to the sulfur (oxygen) atom. This fact suggests that the carbon atom induces a trans effect stronger than that due to the sulfur atom. Our computational method does not allow a rigorous analysis both because the parameters used are not completely reliable and because the lack of high symmetry allows a great deal of orbital mixing. However we have observed that for the model compound $(PH_3)_2NiCS_2$ the two Ni–P overlap populations, practically equal for $\beta = 0°$, become asymmetrical when β changes. For positive β values, the diversification is in the direction of the experimental data. Further support for the idea of a correlation between the rocking of CS_2 and the metal ligand overlap population comes from the geometric parameters of structure (**5**),[8d] which show a slightly negative β value (ca. −2°). Indeed we find a reverse trend: the Fe–C (CO) distance trans to the coordinated sulfur atom is some 0.04 Å longer than the other "in-plane" Fe–C (CO) distance.

Let us turn to the computed energetics of this deformation. Although route I leads to optimized η^2 structures not too far from the experimental one both for L_3MCS_2 and L_2MCS_2 compounds, passage over a high-energy col is required. In fact when the isolated linear CS_2 molecule and the metal fragment approach as in **6**, the conformation **13** is attained, which is

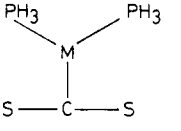

13

ca. 80 kcal/mol more destabilized than the sum of the initial fragment energies. The destabilization of **13** with respect to the optimized η^2 structure is even larger, as expected. Moreover on the downhill side toward the η^2 structure of L_3MCS_2 complexes, a level crossing is encountered. This makes the deformation a forbidden reaction when the HOMO is not fully populated, as in the case of compound **1**.

Although route I seems to be the least motion reaction pathway to the η^2 structure, the results outlined above render its practicability at least questionable. On the other hand, one must also consider the possibility of entering the outlined pathway at a later stage, i.e. by bringing the two fragments to the rendezvous when the angular parameters defined in **7** and **8** are not all zero but θ is already positive (21°, the op-

(14) (a) Grundy, K. R.; Harris, R. O.; Roper, W. R. *J. Organomet. Chem.* **1975**, *90*, C34. (b) Touchard, D.; LeBozec, H.; Dixneuf, P. H. *Ibid.* **1978**, *156*, C29.

(15) (a) Southern, T. G.; Oehmichen, U.; LeMarouille, J. Y.; LeBozec H.; Grandjean, D.; Dixneuf, P. H. *Inorg. Chem.* **1980**, *19*, 2976. (b) Herberhold, M.; Süss-Fink, M.; Kreiter, C. G. *Angew. Chem., Int. Ed. Engl.* **1977**, *16*, 193.

(16) Bianchini, C.; Mealli, C.; Meli, A., to be submitted for publication.

(17) A positive β angle is defined when the rotation brings the coordinated sulfur atom closer to the metal.

(18) Aresta, M.; Nobile, C. F.; Albano, V.; Forni, E.; Manassero, M. *J. Chem. Soc., Chem. Commun.* **1975**, 636.

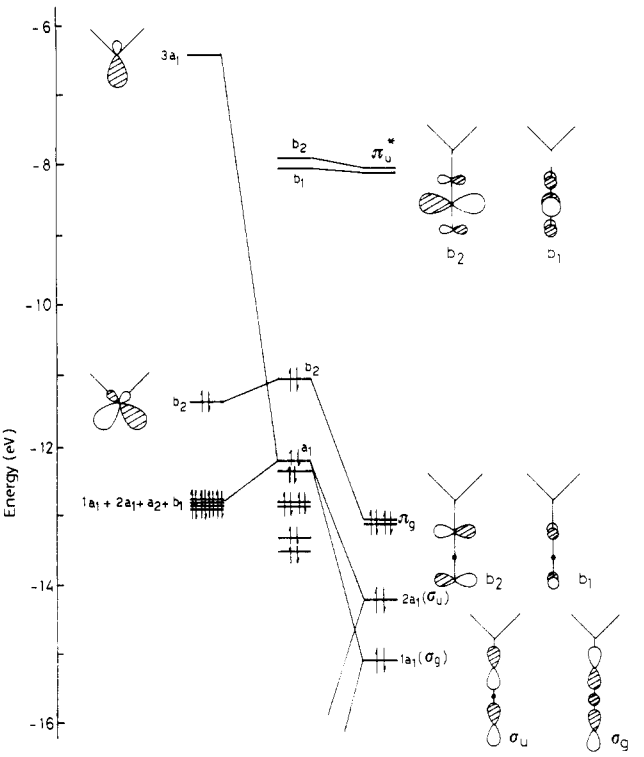

Figure 3. Interaction diagram for the model compound $(PH_3)_2NiCS_2$ with end-on conformation.

timized value). For L_3MCS_2 molecules 1A is already above the 1S level at this point and no crossing is encountered. However in any case, the destabilization of the system with respect to the separate fragments is still very high (of the order of 40–50 kcal/mol).

On the other hand, we calculate energy minima for the end-on mode, **2**, for both L_2MCS_2 and L_3MCS_2 models. The depths of these minima are very close to those calculated for the η^2 mode. This raises the question why no structural evidence for end-on conformation has ever been observed. Before trying an explanation, let us examine some details of the calculations performed along route II.

Route II. Figure 3 shows a diagram for the interaction of a $(PH_3)_3Ni$ fragment with the linear end-on coordinated CS_2 molecule.

In practice all of the bonding comes about from the electron donation of the CS_2 σ_g and σ_u orbitals into the empty metal $3a_1$ orbital. The "in-plane" interaction between the metal orbital and the CS_2 lone pair combination of b_2 symmetry is four-electron destabilizing. As anticipated, this model corresponds to a minimum of the energy, whereas the overlap population between the two fragments is almost 25% less than that found for th η^2 structure optimized through route I.

The shift of the linear CS_2 molecule off the twofold axis, but still parallel to it, is costly in terms of energy: about 10 kcal/mol for an ω angle of 20° (see **9** and **10** for the definition of the parameters). Conversely the rotation of the linear CS_2 molecule pivoted at the coordinated sulfur atom costs little energy in the ρ range 180–98°. Beyond the latter limit the total energy curve becomes rather steep.

Figure 4 shows a series of these energy curves monitored at different values of ω. The trend is very much the same at various ω. The larger the ω, the more rapidly the Ni–C distance shortens. From a certain point on, the CS_2 molecule starts kinking. The transformation of the molecule to such a point requires some activation energy, which may be recovered with kinking.

Figure 5 (solid line) shows the energy variations involved in the three steps outlined above. The depth of the minimum

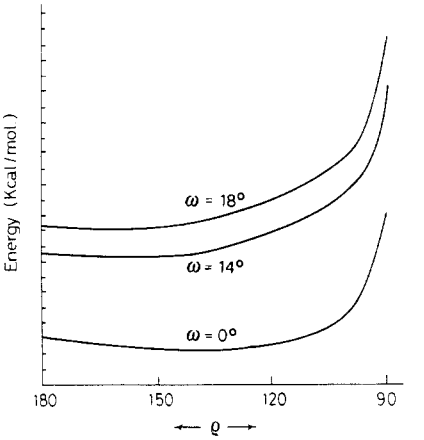

Figure 4. Total energy variation in the $(PH_3)_2NiCS_2$ molecule for rotating the linear S–C–S fragment in the molecular plane. The curves are calculated for different initial shifting of S–C–S off the P–Ni–P bisector. See **9** for definition of the angular variables.

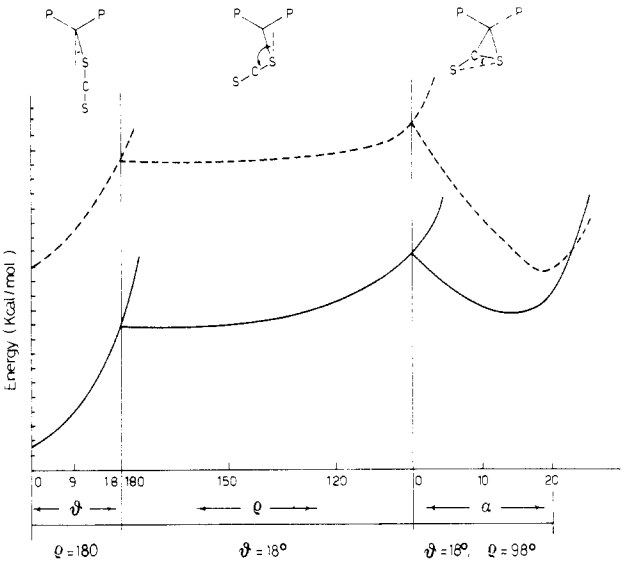

Figure 5. Total energy variation in the interconversion process within the $(PH_3)_2NiCS_2$ model, moving from an end-on to a side-on mode. The angular parameters are defined in **9** and **10**. The solid line refers to a model where the two C–S distances are fixed at 1.60 Å; the dashed line refers to C–S distances equal to 1.65 Å.

on the side of the η^2 conformation is very much dependent on the geometric and energetic parameters used in the calculations. We will show later that in the case of CO_2 complexes the energy keeps going down in the third step, even when the M–C distance becomes so short to be physically unreasonable and no minimum is reached.

The identification of the parameters that affect so greatly the calculations is important in order to understand the geometry and the chemistry of these complexes. In fact, if the loss of energy on bending the CS_2 molecule is overriden by the energy gained through formation of a stronger bond to the metal, the side-on conformation may be reasonably expected.

The orbitals of triatomic molecules have been studied in detail with quite sophisticated methods.[13,19] In particular, the orbital effects on bending these molecules have been established and cautions have been given about the importance of the interelectronic repulsion and the internuclear interaction between terminal atoms.[20] The latter effect is simulated at best poorly by the extended Hückel method, whereas four-

(19) For an exhaustive reference list see: Mulliken, R. S.; Ermler, W. C. "Polyatomic Molecules"; Academic Press: New York, 1982.
(20) Buenker, R. J.; Peyerimhoff, S. D. *Chem. Rev.* **1974**, *74*, 127.

electron destabilization effects help in stopping nonbonded atoms from getting too close. It is mainly for this reason that we observed a minimum φ angle of 150° along route I and that along route II the minimum kinking α angle is optimized at 15°, which again corresponds to a S–C–S angle of 150°. Moreover, the repulsion between lone pairs on sulfur atoms keeps the minimum for side-on conformation higher than that for end-on conformation. In other words, the sulfur–sulfur repulsion seems to be overestimated by our calculations whereas the calculations underestimate the oxygen–oxygen repulsion in the CO_2-containing models.

The critical MO for a CX_2 molecule is that corresponding to the "in-plane" combination of lone pairs on terminal atoms. For $D_{\infty h}$ symmetry (linear molecule), this MO (π_g) is composed of pure p_z atomic orbitals, but when the molecule bends (b_2), some p_x character mixes in, thus reorienting the lone pairs, **14**. It is just the increasing negative overlap population

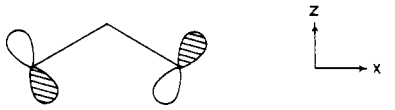

14

between these p_x orbitals that greatly destabilizes the corresponding level and increases the total energy as well. The atomic orbitals in **14** are more diffuse in CS_2 than in CO_2, and consequently the total energy of CS_2 is estimated to increase much more rapidly than that of CO_2 on C_{2v} distortion.

One possibility for achieving a better match between calculations and experiment is that of empirically adjusting the exponents of the terminal atom p orbitals. We avoided this procedure, instead trying some geometrical modifications on CS_2. The C–S distances, which earlier had been kept fixed at 1.60 Å, were lengthened to 1.65 Å. In this manner the overlap between the sulfur p_x orbitals is decreased and their repulsion softened. What is remarkable is that the energy curve for kinking (Figure 5, dashed line) shifts the minimum toward S–C–S angles that are closer to experiment (ca. 140°), and the depth of the minimum is beyond that of the end-on conformation.

If L_3MCS_2 models are calculated, it is noteworthy that the nature of the HOMO is at no point along the route changed.

All this means that route II is a reasonable reaction path for switching from an end-on to a side-on conformation. The lengthening of the C–S distances is a crucial but not totally artificial point. In fact the 1.60-Å choice was initially nothing more than a compromise between the 1.55-Å bond in free CS_2 and the upper limit (1.65 Å) for the average of the C–S bonds in structures **1–5**.

In summary, we believe that the bonding of CS_2 to a metal fragment proceeds through an approach of type **5** with the initial formation of the η^1 end-on mode. Although on the other side of the col (η^2 coordination) the energy minimum is not much deeper (only a few kcal/mol preference is calculated), the electrophilic carbon atom has the possibility of quenching its thirst for electrons by activation of the back-bonding mechanism from the metal. For this reason the system may actually bypass the energy barrier, which is not too high in any case (ca. 10 kcal/mol).

It is now interesting to see how the above analysis compares with some of the suggestions proposed by other authors in terms of valence-bond canonical representations of the bonding.[3]

Since on the basis of electronegativity arguments the π_u set of CS_2 is more centered on sulfur, whereas the π_u^* partner is centered on carbon (see Figure 3), the former atom is more involved in donation and the latter in back-donation. Moreover, back-donation is by far most important for the overall bonding in the molecule due to the smaller energy gap between the interacting fragment orbitals. Accordingly **15** seems more appropriate than **16** for a description of the bonding.

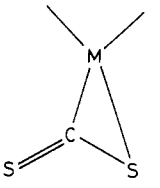

15

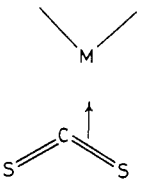

16

It has also been stressed, and the calculations have confirmed, that charge accumulates on the uncoordinated sulfur atom, which may eventually undergo an electrophilic attack. Two alternative zwitterionic descriptions have been proposed: **17** and **18**.[3a] The M=C double bond in **18** is questionable,

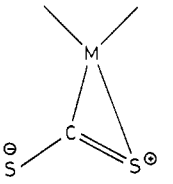

17

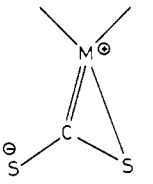

18

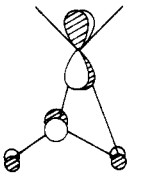

19

because we have found that the second CS_2 π_u^* orbital does not significantly overlap with any filled metal orbital of A symmetry, as shown in **19** Any other interaction of lower CS_2 π orbitals are four-electron destabilizing. On the other hand, structure **18** was proposed to rationalize the shorter M–C distances in these complexes compared with those found in η^2 acetylene and olefin complexes.[8d] Instead we suggest that the strength of the metal–carbon bond is a consequence of the prevailing involvement of the carbon orbital in π back-donation, following the electronegativity arguments mentioned earlier.

Complexes with Carbon Dioxide

It appears that carbon dioxide is more reluctant than carbon disulfide to bond a transition-metal fragment. Beside the compound Co(pr-salen)KCO_2THF (**7**),[9] whose skeleton is shown in **4**, the other examples of complexes containing CO_2 are the compound $(C_5H_4Me)_2NbCO_2$ (**8**)[21] and compound **6**.[18]

We have repeated for CO_2 models all the calculations already performed for their CS_2 analogues.

In general it is found that the side-on mode is largely stabilized both for $(PH_3)_2NiCO_2$ and $(PH_3)_3NiCO_2$ models. However we cannot optimize the O–C–O angle since the energy drops with no arrest, whatever the mechanism (route I or route II) that allows bending of carbon dioxide. Disregarding route I, which also in this case passes a high-energy region at the intermediate stage of type **13**, let us examine some details of route II.

Figure 6 shows a plot of the total energy along the main stages of the path. The diagram differs slightly from the CS_2 case, Figure 5, in that here the initial approach of the two interacting fragments, brought together from infinity, is plotted at the left side of figure. This is to make the point that the end-on structure is not actually an energy minimum as it happens for CS_2. The end-on conformer is indeed less stable than the isolated fragments. Qualitatively, second-order perturbation arguments[22] are sufficient to rationalize this fact. With respect to the interaction diagram of Figure 3, there is

(21) Bristow, G. S.; Hitchcock, P. B.; Lappert, M. F. *J. Chem. Soc., Chem. Commun.* **1981**, 1145.
(22) Hoffmann, R. *Acc. Chem. Res.* **1971**, *4*, 1.

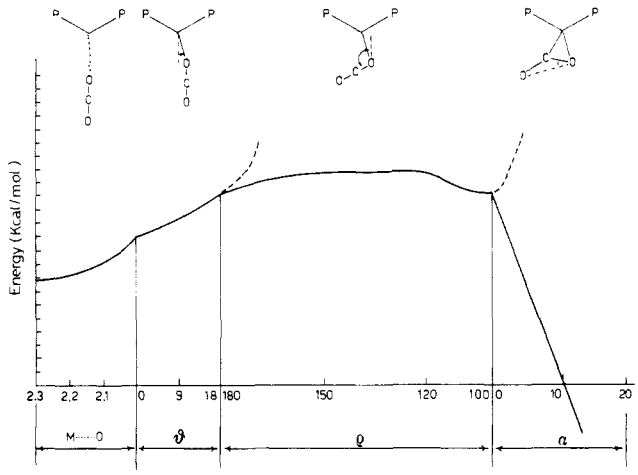

Figure 6. Total energy variation along the pathway that brings a linear CO_2 molecule and a $(PH_3)_2Ni$ fragment, noninteracting, to the geometry of an end-on complex and hence to the side-on complex. The angular parameters are defined in **9** and **10**.

a much larger energy gap between the empty metal $3a_1$ orbital and the CO_2 σ_u and σ_g orbitals. The latter are indeed lower in energy since oxygen is more electronegative than sulfur. Moreover, the oxygen atomic orbitals are more contracted than those of sulfur and so are σ_u and σ_g. The result is a smaller overlap with the metal $3a_1$ level. The M–CO_2 σ bond, if any, does not sufficiently stabilize the complex, which suffers destabilizing four-electron interactions between CO_2 lone pairs and filled metal π orbitals. Thus, the extended Hückel method indicates the instability of the end-on conformation, although quantitatively the numbers are too small to be very reliable.

However, the recent ab initio results by Sakaki, Kitaura, and Morokuma for d^{10} $(PH_3)_2MCO_2$ complexes[5] show that the stability of the end-on conformation is strongly dependent on interactions of electrostatic origin (not well accounted for by EH). Only coordination by a positively charged metal ion such as Cu(I) may provide sufficient electrostatic stabilization for the end-on mode. Conversely the side-on mode is favored for the $(PH_3)_2NiCO_2$ molecule.

Although in terms of the EH method the formation of the end-on conformer costs little energy, the initial repulsion of the metal and CO_2 fragments may well be at the origin of their relatively scarce interaction.

Once the end-on conformer is formed, route II may be accessed. However, as anticipated, the complex does not find an energy minimum for kinking of CO_2; that is to say that the EH method is not able to optimize the η^2 structure. The energy parameters used for oxygen[23] are probably not sufficiently good, and, in contrast with the CS_2 case, no adjustment of geometrical parameters provides results as good here. Evidently the interaction energy between the two fragments is at no point properly matched by the energy spent for CO_2 deformation. The oxygen orbitals are too contracted, and the shrinking of the C–O distances from 1.20 (value used for the plot of Figure 6) to 1.16 Å (the distance in the free linear CO_2 molecule) does not introduce sufficient repulsion. We did not use smaller values that would have been unrealistic. We recall at this point that the use of ab initio methods gives a very realistic binding energy curve for the bending of CO_2 in $(PH_3)_2NiCO_2$.[5] On the other hand, the EH analysis clearly indicates where the different behavior of CO_2 relative to CS_2 originates from. One must refer back to **11**, the three orbitals

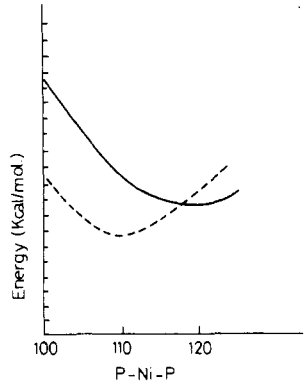

Figure 7. Total energy variation in $(PH_3)_2NiCO_2$ (solid line) and in $(PH_3)_2NiCS_2$ (dashed line) as a function of P–Ni–P angle. The two curves are superimposed on a arbitrary energy scale.

interaction giving rise to the HOMO in these molecules. In CS_2 complexes the percentage contribution of b_2 and a_1 orbitals is approximately equal, whereas in CO_2 compounds the HOMO consists almost entirely of the bonding combination of the metal S and CO_2 a_1 orbital. The mixing of b_2 in antibonding fashion vanishes. Thus, the destabilizing effect of the terminal-atom lone pairs, b_2, is greatly reduced in this case.

When the structures of L_2MCS_2 complexes[8a,b] are compared with that of the complex $(PCy_3)_2NiCO_2$,[18] the P–M–P angle is found to be 12–15° smaller in the former. Figure 7 shows the total energy variation as a function of this angle for both CS_2 and CO_2 models. The geometry of the CX_2 fragment was kept close to the experimental one in either case. The two curves have minima at angles in nice agreement with the structural data. It is not difficult to rationalize this fact: when a p orbital mixes in a d orbital the "bite" of the latter is increased and this may eventually become too large for overlapping well with a π^* orbital of CO_2 that, due to the short C–O distance, also has a small "bite". The situation is depicted in **20**. Similar interligand angle effects have been previously discussed in some detail.[24]

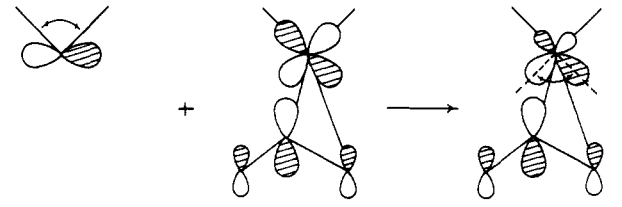

20

The above arguments may account for the unique stability of compound **6**.[18] In fact, as has been pointed out, the presence of the bulky cyclohexyl substituents at the phosphines appears mandatory in order to stabilize the CO_2 adduct. Less hindered substituents do not force the P–Ni–P angle to stay open sufficiently, thus causing a net loss of overlap between the interacting fragment orbitals. The latter requirement adds to the previously mentioned difficulties that stand in the way of CO_2 attaining end-on coordination to the metal, i.e. the initial step toward η^2 coordination.

There may be other factors, but we believe that these arguments rationalize the paucity of the known adducts of CO_2, compared to those of CS_2. Moreover they also suggest that COS adducts should prefer C–S rather than C–O η^2 coordination, as seems to be the case.[2f]

(23) The parameters for oxygen, carbon, hydrogen, phosphorus, sulfur, and cobalt atoms are the same as those reported in: Pinhas, A. R.; Hoffmann, R. *Inorg. Chem.* **1979**, *18*, 654. The parameters for nickel and nitrogen atoms are those given in: Albright, T. A.; Hoffmann, R.; Thibeault, J. C.; Thorn, D. L. *J. Am. Chem. Soc.* **1979**, *101*, 3801.

(24) (a) Yoshida, T.; Tatsumi, K.; Matsumoto, M.; Nakatsu, K.; Nakamura, A.; Fueno, T.; Otsuka, S. *Nouv. J. Chim.* **1979**, *3*, 761. (b) Yoshida, T.; Tatsumi, K.; Otsuka, S. *Pure Appl. Chem.* **1980**, *52*, 713. (c) Mealli, C.; Midollini, S.; Moneti, S.; Albright, T. A. *Helv. Chim. Acta*, in press.

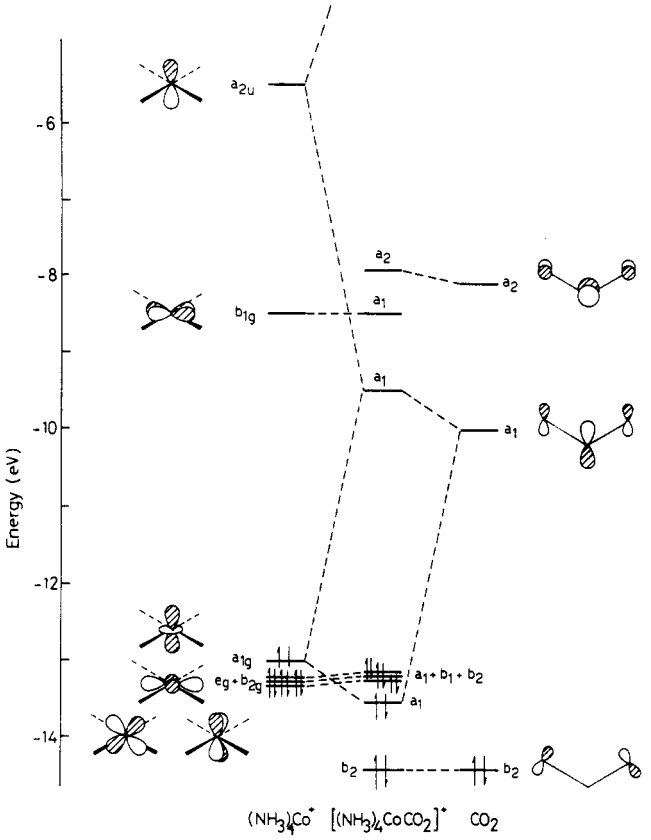

Figure 8. Interaction diagram for the model $(NH_3)_4CoCO_2^+$ with Co–C coordination.

One of the three known crystal structures of CO_2 complexes is sketched in **4** (compound **7**[9]). It is an unique example of metal–C coordination and it has been also called "supported CO_2 coordination"[2e] since there is an additional labile interaction with the potassium cations merged into the complex framework. Disregarding for the moment this latter aspect, is the L_4MCO_2 fragment sufficiently stabilized only by electronic effects? The d^8-L_4M fragment is different from any fragment considered till now. It must be considered a stable saturated square-planar 16-electron species.[11b] The MO levels of a square-planar $(NH_3)_4Co^+$ model are shown at the left side of Figure 8. At high energy and empty is the *xy* orbital. The HOMO is essentially the z^2 orbital hybridized with some mixing of metal s; as a result, **21**, the lobes along the fourfold

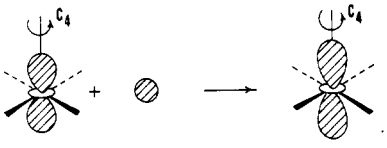

21

axis are expanded. Thus, the orbital in question interacts better with the CO_2 a_1 (π_u^*) orbital. This interaction is a donation from the metal, while the back-donation from CO_2 is practically nonexistent. However enough bonding and electronic stabilization are conferred to the complex as confirmed by a fairly large overlap population between the fragments and a stabilization of about 25 kcal/mol with respect to the sum of the energies of the isolated fragments.

Concerning the formation of the complex, since both approaches **5** and **6** seem unfavorable, the presence of the K^+ cations seems essential for anchoring the CO_2 molecule, which then may be thought of as being attacked by the L_4M fragment.

At least one other, indirect, example of coordination mode **3** is available. The complex $[Ir(dmpe)_2Cl(CO_2Me)]FSO_3$[25a] (**9**) is the methylated derivative of the complex $Ir(dmpe)_2Cl(CO_2)$[25b] (**10**) (dmpe = $Me_2PCH_2CH_2PMe_2$). The structure of **9** shows M–C coordination, which is probably present in **10** as well, **22**. A structure of type **22** was recently ascertained for $[Rh(diars)_2ClCO_2]$, isoelectronic with **10**.[26]

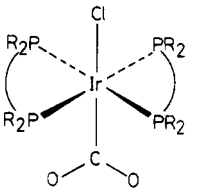

22

Further support for the idea of C coordination in **10** comes from the CO_2 IR bands that are intrinsically different from those obtained for compound **6** where CO_2 is η^2 bonded. The P_4ClIr (I) fragment already has 18 electrons. It is essentially an octahedron with one empty coordination site. Under these circumstances there is a metal lone pair suitable for donation to the CO_2 carbon atom orbital in a_1. Notice that, when the fragment P_4ClIr has one phosphine molecule missing, one observes the formation of head-to-tail C_2O_4 grouping. In practice two CO_2 molecules enter the coordination sphere of the metal, **23**.[27] In this manner the d^{18}-L_5M fragment is

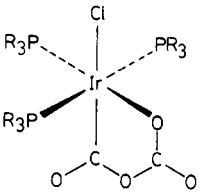

23

restored through σ donation from one oxygen atom. Metal to carbon donation at the sixth vertex of the octahedron is once again possible. A completely analogous situation is found in the carbon disulfide complex $(C_5H_5)Rh(PMe_3)C_2S_4$[28] (**11**).

All these examples are suggestive of the following generalization: coordination mode **3** of CX_2 molecules is attainable when the metal atom is electronically saturated by its coligands and the fragment has a free coordination site. Nonetheless the initial approach of the two fragments may be difficult and the reaction may be greatly facilitated if $CO_2(CS_2)$ is kept in place by a second function having ionic character.

Fluxionality in CO_2 and CS_2 Complexes

Our MO analysis provides some hints concerning the interpretation of available NMR data for η^2-bonded heteroallene molecules.

The question is whether the CX_2 molecule is rigid or rotating around the axis passing through the metal and the coordinated C–X bond. We know for example that complexes of the type L_2MCS_2 are not fluxional whereas L_2MCO_2 complexes are.[2f,29] In the complex $(C_5H_5)Rh(PMe_2Ph)CS_2$ (12),[2g] CS_2 is rigid

(25) (a) Harlow, R. L.; Kinney, J. B.; Hershovitz, T. *J. Chem. Soc., Chem. Commun.* **1980**, 813. (b) Herskovitz, T. *J. Am. Chem. Soc.* **1977**, *99*, 2391.
(26) Herskovitz, T.; Calabrese, J. C.; Kinney, J. B. "Abstracts of Papers", 185th National Meeting of the American Chemical Society, Seattle, WA, March 1983; American Chemical Society: Washington, DC, 1983; INOR 297.
(27) Herskovitz, T.; Guggenberger, L. J. *J. Am. Chem. Soc.* **1976**, *98*, 1615.
(28) Werner, H.; Kolb, O.; Feser, R.; Shubert, U. *J. Organomet. Chem.* **1980**, *191*, 283.
(29) Mason, M. G.; Ibers, J. A. *J. Am. Chem. Soc.* **1982**, *104*, 5153.

while it is not in the complex $(C_5H_5)Mn(CO)_2CS_2$ (**13**).[14b]

Most significant to the interpretation of these facts is the π type back-bonding interaction between the filled metal d orbital and the empty, in-plane, π^* orbital of CS_2, **24**. If the

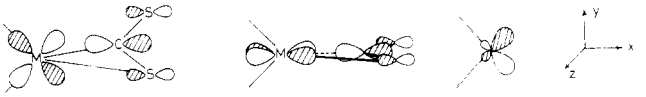

24 25 26

metal fragment has a perpendicular d_π orbital, **25**, that is close in energy and similar in shape to the one shown in **24**, the rotation of CX_2 is not expected to be hindered.

Let us consider the L_2M fragment. We know that removal of two ligands from a square-planar complex hybridizes the *xy* orbital, **26**, but it does not affect the *xz* orbital. Moreover the *xy* orbital fails in energy because of the missing ligands but usually stays above that of the *xz* orbital. These arguments suggest that the interaction of L_2M with CS_2, in an upright orientation, is unfavorable. The calculations show that the barrier to rotation is high, ca. 30 kcal/mol for the optimized $(PH_3)_2NiCS_2$ model. However, we find that the magnitude of the barrier to rotation is dependent on the value of the P–Ni–P angle. The more open this angle, the less hybridized is *xy* and the more similar (in energy and shape) is the orbital to *xz*. We have mentioned above how the latter angular parameter affects the stability of the $(PH_3)_2NiCO_2$ model. However we find that if the experimental value of 120° is used,[18] the hindered rotation of CO_2 has a barrier that is about half that of CS_2; the barrier increases rapidly on closing the P–Ni–P angle and, at values of 105–110°, the barrier is of the same magnitude as was found for the CS_2 model.

In **12** the metal fragment can be described as d^8-L_4M, isolobal with d^{10}-L_2M. It follows that what was said above about the fluxionality of L_2MCX_2 complexes holds for **12** as well and indeed the molecule is rigid.

The isolobal analogy,[12] **27**, is extended to d^6-L_5M fragments;

$$d^8\text{-}L_4M \longleftrightarrow d^{10}\text{-}L_2M \longleftrightarrow d^6\text{-}L_5M$$

27

the latter has a high-energy empty σ orbital and three low-filled orbitals (two π and one δ), the remnants of the t_{2g} octahedral set. Important to our discussion is the full equivalence of the two orthogonal orbitals appropriate for back-donation. The fragment $(C_5H_5)(CO)_2Mn$ is reducible to the ideal d^6-L_5M fragment, and indeed we know from experiment that complex **13** is fluxional.[15b]

Also, d^{10}-L_3M fragments, although not actually isolobal with those in **27**, have one empty σ orbital and two degenerate π orbitals (somewhat tilted) that should favor fluxionality. Indeed our calculations do not predict any apprciable barrier for rotation of CX_2 molecules η^2 bonded to L_3M fragments. Unfortunately there are no $^{31}P\{^1H\}$ NMR data available for (triphos)MCS_2 (M = Ni, Co) to confirm the prediction. (Triphos)M fragments undergo free rotation about the pseudo-threefold axis, thus rendering the three phosphorus atoms equivalent.[30] The interpretation of the NMR spectra is unwieldy under these circumstances.

A final comment relates to the possibility of different fluxional mechanisms such as that shown in **28**. Calculations performed along route I showed that, for any φ angle, the most destabilized structures are found at θ = 0° (see **7** for the definitions of θ and φ). In no case is the destabilization energy less than 30 kcal/mol, both for L_2NiCS_2 and L_3NiCS_2 models. The reason for this is that the most important bonding interaction, i.e. π back-bonding, is absent for symmetric coordination of CS_2 to the metal (see Figure 1). Accordingly the seemingly simple mechanism **28** appears unlikely.

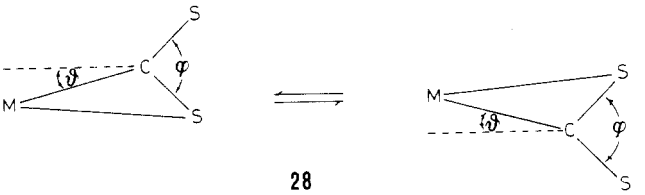

28

Conclusions and Extensions

Not all of the aspects of the electronic stability in complexes containing CO_2, CS_2, or COS molecules can be elucidated with a study of this type. Beside the well-known limits of the computational method, the lack of high symmetries often makes the analysis of the orbital interactions a difficult task. Nonetheless, some understanding of the factors governing bonding in these compounds has been achieved.

The coordination of a CX_2 molecule to a metal fragment that has two electrons less than the closed-shell configuration is likely to start from the end-on mode. Interconversion to a side-on geometry can follow with relative ease. In this state back-donation from the metal satisfies the electrophilic character of carbon, whereas donation from CX_2, mainly through the coordinated X atom, still provides a closed-shell configuration to the metal.

Conversely, the requirement for a CX_2 molecule to attain C coordination seems to be set by the closed-shell configuration of the metal fragment itself and by the presence of a free coordination site. But even in this case the complex is not easily obtained. The *rendezvous* of the fragments after an approach either of type **5** or type **6** is made difficult by repulsive forces. The additional requirement is the anchoring of the initially linear CX_2 molecule close to the metal.

Alternatively we suggest that the interaction between the fragments can be made possible if CX_2 is promoted to an excited state that bends the molecule (notice that the occupation of the "in-plane" π_u^* orbital favors bending.

Our analysis of the bonding also contains some hints for interpreting the reactivity of CX_2 complexes toward both electrophilic and nucleophilic agents. For example, we have seen that the former agents can attack the uncoordinated sulfur (oxygen) atom in side-on conformers. Recall that π back-donation from metal is quite effective and that, at least for CS_2, the mixing of the sulfur lone-pair combination in the HOMO, **11**, magnifies both the extension and the electron population of this reactive orbital just at the uncoordinated atom. The reactivity of that atom toward σ acceptors follows in obvious fashion.

We have seen that the interconversion from end-on to side-on coordination should be relatively facile, with an energy barrier that is not too high. Thus, the side-on-coordinated CX_2 molecule can undergo a backward motion, which unfastens the carbon atom, stretches the triatomic molecule, anchored at the metal through one X atom, and finally rotates it back to the end-on conformer. During this process an intermediate similar to the one depicted in **9** can undergo nucleophilic attack at carbon.

As an example **1** is reactive toward elemental sulfur and selenium, yielding compounds of type **29**.[31] The reaction

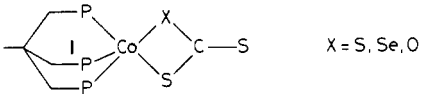

29

(30) Bianchini, C.; Innocenti, P.; Meli, A. submitted for publication in *J. Chem. Soc., Dalton Trans.*

(31) Bianchini, C.; Meli, A. *J. Chem. Soc., Chem. Commun.*, in press.

becomes understandable if the mechanism outlined above is considered: the nucleophilic attack at the carbon atom of the linear CS_2 bends the CS_2 fragment, because the electrons donated enter a π_u^* orbital that is stabilized on bending. The coordination of X to the metal ensues.

The presence of intermediates of type **9** gains greater credibility if the reactions leading to head-to-tail coordination of C_2X_4 clusters,[27,28] **23**, are examined. Referring to the end-on/side-on interconversion mechanism, the formation of compound **11** from the complex $(C_5H_5)Rh(Me_3P)CS_2$ and excess CS_2 seems reasonable. The three steps are depicted in **30**.

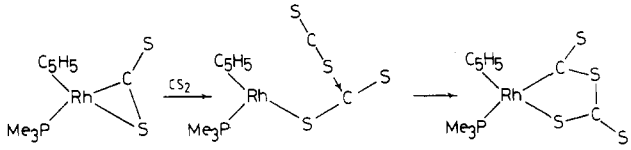

30

The examples reported above are just a few from the rich and diverse chapter of the reactivity of complexed CS_2 and CO_2 molecules. It is clear that much deeper insight into the mechanism of each specific reaction is needed. Theoretical investigation is still scarce in this field.

Acknowledgment. C.M. and R.H. are grateful to NATO for awarding a research grant (No. 200.81) through which this collaborative project was made possible. R.H. acknowledges National Science Foundation support (Grant CHE 7828048). Thanks are due to Franco Cecconi for assistance in making drawings. C.M. thanks his CNR colleagues for continuous and helpful discussions.

Appendix

The extended Hückel calculations[6] utilized a modified version of the Wolfsberg-Helmholz formula;[32] see ref 23 for information relative to the atomic parameters used.

The PH_3 molecules had P-H bonds of 1.4 Å and H-P-H angles of 109.5°. In NH_3 molecules the N-H distances were fixed at 1.1 Å. In the $(PH_3)_3Ni$ fragment, the P-Ni-P angle was 90°. In the $(PH_3)_2Ni$ fragment the P-Ni-P angle was 107° unless otherwise specified in the text. All the Ni-P distances were kept fixed at 2.25 Å. In the model $(NH_3)_4CoCO_2^+$, the Ni-N distances were 2.0 Å.

Registry No. $(PH_3)_3NiCS_2$, 87761-75-9; $(PH_3)_2NiCS_2$, 87761-76-0; $(PH_3)_2NiCO_2$, 79953-45-0; CO_2, 124-38-9; CS_2, 75-15-0.

(32) Ammeter, J. H.; Bürgi, H.-B.; Thibeault, J. C.; Hoffmann, R. *J. Am. Chem. Soc.* **1978**, *100*, 3686.

Contribution No. 6540 from the Division of Chemistry and Chemical Engineering, California Institute of Technology, Pasadena, California 91125

Ruthenium Complexes of 1,3-Bis(2-pyridylimino)isoindolines as Alcohol Oxidation Catalysts

ROBERT R. GAGNÉ* and DAVID N. MARKS

Received January 21, 1983

The ruthenium complex (1,3-bis(4-methyl-2-pyridylimino)isoindoline)trichlororuthenium(III) catalyzes the autoxidation and electrochemical oxidation of alcohols in basic alcoholic solution. The reaction is general, resulting in the oxidation of primary and secondary alcohols, with the principal products being aldehydes and ketones. The catalytic autoxidation is affected by the strength of the base used and its coordinating ability. The best results were obtained with sodium ethoxide as a base. Turnover numbers of 10-30 per day were observed in 1 atm of oxygen at ambient temperature, with larger turnover numbers at higher temperatures. More than 200 turnovers were observed in the oxidation of ethanol at the ambient temperature with little or no loss of catalytic activity. The catalyzed electrochemical oxidation was carried out in an alcoholic solution containing 2,6-lutidine with a carbon electrode at 0.8-1.0 V vs. NHE. In the absence of catalyst, negligible current was observed. More than 20 catalytic cycles were completed with the current remaining at 75% of its initial value. The ruthenium(III) complex exhibits reversible one-electron oxidation waves in non-alcoholic solvents in the presence or absence of 2,6-lutidine. Possible pathways for the catalytic autoxidation and electrochemical oxidation are presented.

Introduction

High-oxidation-state transition-metal complexes, such as MnO_4^- and CrO_3, are commonly used reagents for the oxidation of alcohols. These complexes, however, often show limited selectivity in their reactions and function, in normal use, as stoichiometric oxidizing agents.[1]

Few transition-metal complexes are known that catalyze the oxidation of alcohols, and in most cases, the reaction mechanisms are not well understood.[2-8] We report the oxidation of alcohols to aldehydes or ketones by molecular oxygen, as mediated by a ruthenium catalyst in homogeneous solution. The oxidation takes place in a basic alcoholic solution of the Ru(III) complex containing ligand **1**, (4′-MeLH)$RuCl_3$. In addition the Ru(III) complex catalyzes the electrochemical oxidation of both primary and secondary alcohols. The catalytic oxidations were studied to define the scope and possible mechanism of these reactions.

Results and Discussion

Characterization of (4′-MeLH)$RuCl_3$. The synthesis of (4′-MeLH)$RuCl_3$ has been reported earlier.[9] The Ru(III)

(1) House, H. O. "Modern Synthetic Reactions", 2nd ed.; W. A. Benjamin: Reading, MA, 1972.
(2) Tang, R.; Diamond, S. E.; Neary, N.; Mares, F. *J. Chem. Soc., Chem. Commun.* **1978**, 562.
(3) Dobson, A.; Robinson, S. D. *Inorg. Chem.* **1977**, *16*, 137.
(4) Murakata, M.; Nishibayashi, S.; Sakamoto, H. *J. Chem. Soc., Chem. Commun.* **1980**, 219.
(5) Blackburn, T. F.; Schwartz, J. *J. Chem. Soc., Chem. Commun.* **1977**, 157.
(6) Roundhill, D. M.; Dickson, M. K.; Dixit, N. S.; Sudha-Dixit, B. P. *J. Am. Chem. Soc.* **1980**, *102*, 5538.
(7) Bibby, C. E.; Grigg, R.; Price, R. *J. Chem. Soc., Dalton Trans.* **1977**, 872.
(8) Tovrog, B. S.; Diamond, S. E.; Mares, F.; Szalkiewicz, A. *J. Am. Chem. Soc.* **1981**, *103*, 3522.

0020-1669/84/1323-0065$01.50/0